CD68 acts as a major gateway for malaria sporozoite liver infection

Sung-Jae Cha,[1,2] Kiwon Park,[1,2] Prakash Srinivasan,[4] Christian W. Schindler,[5,6] Nico van Rooijen,[7] Monique Stins,[3] and Marcelo Jacobs-Lorena[1,2]

[1]W. Harry Feinstone Department of Molecular Microbiology and Immunology and [2]Johns Hopkins Malaria Research Institute, Bloomberg School of Public Health; and [3]Department of Neurology, Johns Hopkins School of Medicine, Johns Hopkins University, Baltimore, MD 21205
[4]Laboratory of Malaria and Vector Research, National Institute of Allergy and Infectious Diseases, National Institutes of Health, Rockville, MD 20852
[5]Department of Microbiology and Immunology and [6]Department of Medicine, Columbia University, New York, NY 10032
[7]Department of Molecular Cell Biology and Immunology, VUmc, 1081 BT Amsterdam, Netherlands

After being delivered by the bite from an infected mosquito, *Plasmodium* sporozoites enter the blood circulation and infect the liver. Previous evidence suggests that Kupffer cells, a macrophage-like component of the liver blood vessel lining, are traversed by sporozoites to initiate liver invasion. However, the molecular determinants of sporozoite–Kupffer cell interactions are unknown. Understanding the molecular basis for this specific recognition may lead to novel therapeutic strategies to control malaria. Using a phage display library screen, we identified a peptide, P39, that strongly binds to the Kupffer cell surface and, importantly, inhibits sporozoite Kupffer cell entry. Furthermore, we determined that P39 binds to CD68, a putative receptor for sporozoite invasion of Kupffer cells that acts as a gateway for malaria infection of the liver.

CORRESPONDENCE
Marcelo Jacobs-Lorena:
mlorena@jhsph.edu

Abbreviations used: CSP, circumsporozoite protein; GAG, glycosaminoglycan; qRT-PCR, quantitative RT-PCR.

Malaria remains one of the world's most devastating diseases, afflicting close to 500 million people and causing nearly 1 million deaths every year. Parasite resistance to drugs is of major concern (White et al., 2014), and new drug targets need to be urgently identified. Some progress has recently been made in malaria vaccine development, but identification of new vaccine targets remains a high priority (Moorthy et al., 2004; Moorthy and Kieny, 2010). A better understanding of parasite infection of the human host is crucial for the development of new tools to fight the disease.

Infection of a vertebrate host is initiated by the bite of an infected female mosquito. Sporozoites released with the mosquito saliva enter the blood circulation and exit in the liver to establish a productive infection. Hepatocyte infection leads to a dramatic amplification of parasite numbers: 1 sporozoite generates up to 10,000 merozoites that are subsequently released into the bloodstream where they continuously propagate inside red blood cells, causing disease symptoms (Sturm et al., 2006). The pre-erythrocytic liver stages represent a severe bottleneck in parasite numbers and constitute a prime target for induction of sterile immunity. Understanding the mechanisms of parasite liver invasion may provide crucial insights for pre-erythrocytic malaria drug and vaccine development.

After delivery by an infected mosquito, sporozoites circulate through the entire body. What cues does the parasite use to exit the blood circulation in the liver and which mechanisms operate for sporozoite exit from the circulation are fundamental questions that are incompletely understood. The liver has specialized blood vessels, the sinusoids, whose walls are made up by two cell types: fenestrated endothelial cells and macrophage-like Kupffer cells (Widmann et al., 1972). Circulating sporozoites are believed to be captured via strong interaction between circumsporozoite protein (CSP), a major sporozoite surface protein, and the highly sulfated heparan sulfate proteoglycans (HSPGs) that are synthesized by stellate cells in the space of Disse

K. Park's present address is Division of Inflammation Biology, La Jolla Institute for Allergy and Immunology, La Jolla, CA 92037.

The Rockefeller University Press $30.00
J. Exp. Med. 2015 Vol. 212 No. 9 1391-1403
www.jem.org/cgi/doi/10.1084/jem.20110575

The Journal of Experimental Medicine

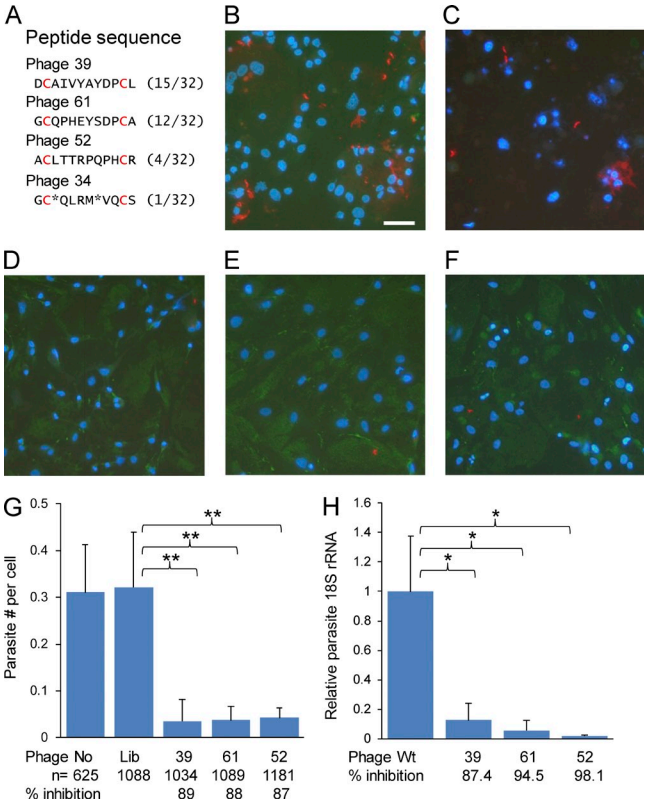

Figure 1. Selected phages inhibit sporozoite entry into Kupffer cells and mouse liver. (A) Predicted amino acid sequence of peptides displayed by phages selected for binding to Kupffer cells. Frequency of each of the four recovered peptides among the 32 phages sequenced is denoted in parenthesis. Asterisks indicate a stop codon. All peptides from this library have a cysteine residue (red) at positions 2 and 11. (B–F) Non-selected library phages (B), PBS buffer only (C), phage 39 (D), phage 61 (E), or phage 52 (F) was added to primary rat Kupffer cell cultures, followed by addition of *P. berghei* sporozoites. After 2-h incubation at 37°C, the cells were fixed, permeabilized, and then incubated with an anti-CSP antibody (red) and an anti-M13 phage antibody (green). Nuclei were stained with DAPI (blue). The anti-CSP antibody detects both attached and invaded sporozoites. Bar, 100 µm. (G) The mean number of sporozoites per cell was measured in 10 fields/well under 200-fold magnification. Data from three independent replicate experiments were combined. "n" indicates the number of cells assayed. The percent inhibition relative to the unselected library phage control group (Lib) is displayed. "No" indicates no phage (PBS buffer control). (H) Each selected phage (compare with A) or wild-type phage (Wt) was injected intravenously (10^{10} phages per mouse) into three mice, followed 5 min later by injection of 2×10^4 *P. berghei* sporozoites. Parasite load in livers was determined 42 h later, and percent inhibition relative to the wild-type phage–treated group is displayed. Data from two replicate experiments were pooled, and each bar represents the mean of six mice. (G and H) P-values (*, $P < 0.05$; **, $P < 0.01$) were calculated using the one-way ANOVA test. Error bars indicate standard deviation.

and protrude into the vascular lumen through endothelial fenestrations (Frevert et al., 1993, 1996; Cerami et al., 1994; Pradel et al., 2002; Coppi et al., 2007). The "gateway hypothesis," which has predominated for several decades, suggests that sporozoites glide along the sinusoid wall until they find a Kupffer cell (Frevert et al., 2005), which they traverse to subsequently infect underlying hepatocytes. This hypothesis was supported by ultrastructural data suggesting that sporozoites specifically traverse Kupffer cells and not endothelial cells (Danforth et al., 1980; Meis et al., 1983; Vreden, 1994; Pradel et al., 2002). The molecular basis for this specific recognition is a key unresolved question of the early stages of *Plasmodium* development in its vertebrate host.

We previously used a phage display library screening strategy to identify receptor–ligand combinations used by *Plasmodium* during its cycle in vector mosquitoes (Ghosh et al., 2001, 2009, 2011). Furthermore, blocking the interactions between parasite ligands and mosquito host cell receptors led to a significant reduction of malaria transmission by mosquitos (Ito et al., 2002). By screening a phage display library, we identified a peptide, P39, that binds to Kupffer cells and, by doing so, inhibits sporozoite entry. Further work determined that P39 interacts specifically with a major Kupffer cell surface protein, CD68, making this a candidate receptor for sporozoite traversal of Kupffer cells and liver infection.

RESULTS

Screening a phage display library for peptides that bind to Kupffer cells

Our experiments were designed to test the following hypothesis. Sporozoite entry of liver Kupffer cells requires the interaction between specific molecules on the Kupffer cell surface (putative receptors) and sporozoite ligands. To test this hypothesis, we screened a phage library (Bonnycastle et al., 1996) that displays random 12–amino acid peptides (estimated library complexity: 1.5×10^9 different peptides) for binding to a highly enriched primary Kupffer cell culture. A total of 2×10^{11} library phages were incubated with a primary Kupffer cell culture (98.5% as estimated by staining with the anti-F4/80 macrophage-specific antibody; not depicted) for 20 min, and unbound phages were removed by thorough washing. Phages that remained bound to the Kupffer cell surface were recovered by adding host *Escherichia coli* cells, followed by propagation of the phages in the added bacteria. This selection was repeated three more times, each time with the enriched phage population of the previous round. After the fourth round, the recovered phages were plated and 32 random colonies were picked for sequencing of the DNA insert. The results are summarized in Fig. 1 A. Close to half of the phages (15/32) displayed the same peptide (P39), whereas the majority of the remaining phages displayed one of two other peptides. Considering the high complexity of the initial phage library, these results suggest that the selected peptides specifically interact with Kupffer cells.

To conduct an initial assessment of the specificity of this interaction, we incubated the selected phages with mixed primary rat liver nonparenchymal cell cultures and measured binding using immunofluorescence assays. The selected phages bound only to Kupffer cells and not to other cell types (not depicted). Specific binding of the selected peptides to Kupffer cells raised two possible scenarios: (1) the peptides bind to a

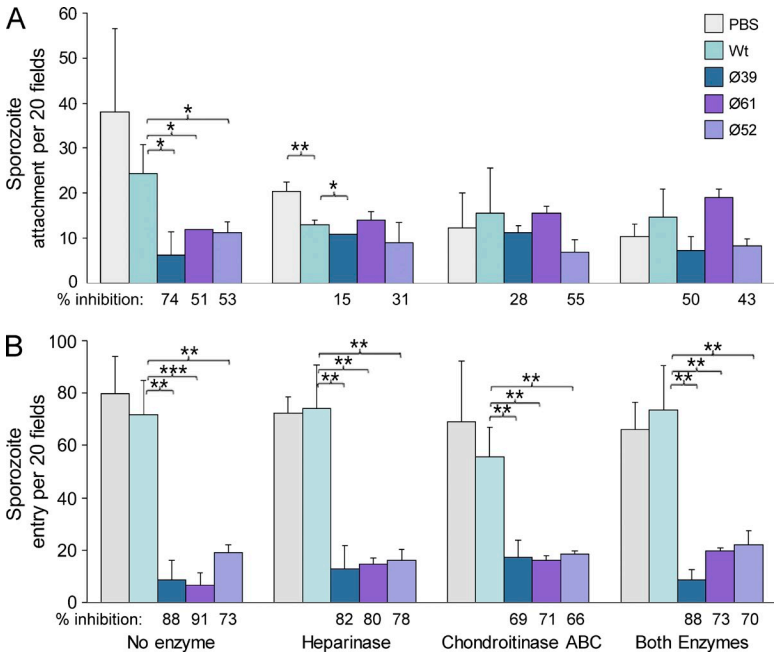

Figure 2. GAG removal does not affect phage inhibition of Kupffer cell entry. (A and B) Primary rat Kupffer cells were either left untreated or treated with the enzymes indicated in the bottom of the figure. This was followed by the sequential addition of the selected phages and *P. berghei* sporozoites. PBS buffer or wild-type phages (Wt) were added as controls. After 2-h incubation at 37°C, unbound sporozoites were washed out and Kupffer cells were fixed for sporozoite counting. The number of attached (A) and intracellular (B) parasites per 20 microscopic fields/well at 400-fold magnification was determined separately. Data from three independent experiments were combined. The percent inhibition relative to the wild-type phage–treated group is displayed at the bottom of each panel. P-values (*, $P < 0.05$; **, $P < 0.01$; ***, $P < 0.001$) were calculated using the one-way ANOVA test. Error bars indicate standard deviation.

putative Kupffer cell receptor for sporozoite entry, or (2) the peptides bind to a Kupffer cell molecule unrelated to sporozoite entry. In the first scenario, peptide binding should result in inhibition of sporozoite entry because peptide occupancy of the receptor would preclude interaction with the presumed sporozoite ligand. In the second scenario, peptide binding should not interfere with sporozoite entry. To distinguish between the two possibilities, the selected phages were added to primary Kupffer cell cultures, followed by incubation with *Plasmodium berghei* sporozoites (Fig. 1). After triple wash, the three selected phages bound to Kupffer cells (Fig. 1, compare green fluorescence background of D–F with C) and strongly inhibited sporozoite interactions with Kupffer cells (Fig. 1, compare number of sporozoites [red] in D–F with B and C; quantified in Fig. 1 G). The green labeling of Kupffer cells in the presence of the nonspecific library phage (Fig. 1, compare B and C) suggests that library phages bound to the Kupffer cell surface, but this nonspecific binding did not interfere with sporozoite interactions (Fig. 1 G). To determine whether the phages also inhibit infection in an in vivo model for *Plasmodium* liver infection, the selected recombinant phages, or wild-type phages as a control, were injected into mice through the tail vein (10^{10} phages/mouse), followed 5 min later by injection of 2×10^4 sporozoites. Parasite liver burden was determined by quantitative RT-PCR (qRT-PCR) after 42 h, as previously described (Bruña-Romero et al., 2001). Relative to the wild-type phage control, the three selected phages strongly inhibited sporozoite liver infection in mice (Fig. 1 H). Together, the results presented to this point support the hypothesis that the peptides displayed by the recombinant phages bind to a Kupffer cell receptor for sporozoite entry.

The P39 peptide binds to macrophage-specific surface proteins, not to glycosaminoglycans (GAGs), and inhibits sporozoite entry into Kupffer cells

To address the nature of the putative Kupffer cell receptor, we sought to determine whether surface GAGs play a role in the inhibition of sporozoite entry by the selected phages. Using experiments that separately assessed sporozoite attachment and entry (Pradel and Frevert, 2001), phage inhibition was compared between Kupffer cells that had been treated or not with enzymes that hydrolyze GAGs (Fig. 2). In agreement with previous studies (Frevert et al., 1996; Pinzon-Ortiz et al., 2001), we found that enzyme treatment decreased sporozoite attachment only for PBS or wild-type phage controls (Fig. 2 A). However, as shown in Fig. 2 B, the recombinant (but not wild-type) phages strongly inhibited sporozoite entry, whether Kupffer cells were pretreated or not with GAG-removing enzymes. The experiments described thus far did not allow the determination of whether inhibition by the recombinant phages is solely caused by the peptides displayed by the phages or whether the phage particles had a contributing role (e.g., steric hindrance). The following experiments made use of a synthetic peptide (termed P39) whose amino acid sequence is identical to the one displayed by phage 39 (Fig. 1 A). The first set of experiments determined that the biotinylated P39 peptide binds to Kupffer cells and that this binding is trypsin sensitive but is not affected by GAG hydrolase treatment (Fig. 3 A), suggesting that P39 binds to a Kupffer cell surface protein. Next we tested whether P39 also binds to other macrophage-like cells by incubating cell lysates with the biotinylated P39 peptide (far-Western blotting). As shown in Fig. 3 B, P39 bound to an ~110-kD protein present only in macrophage-like cell lysates. To localize the

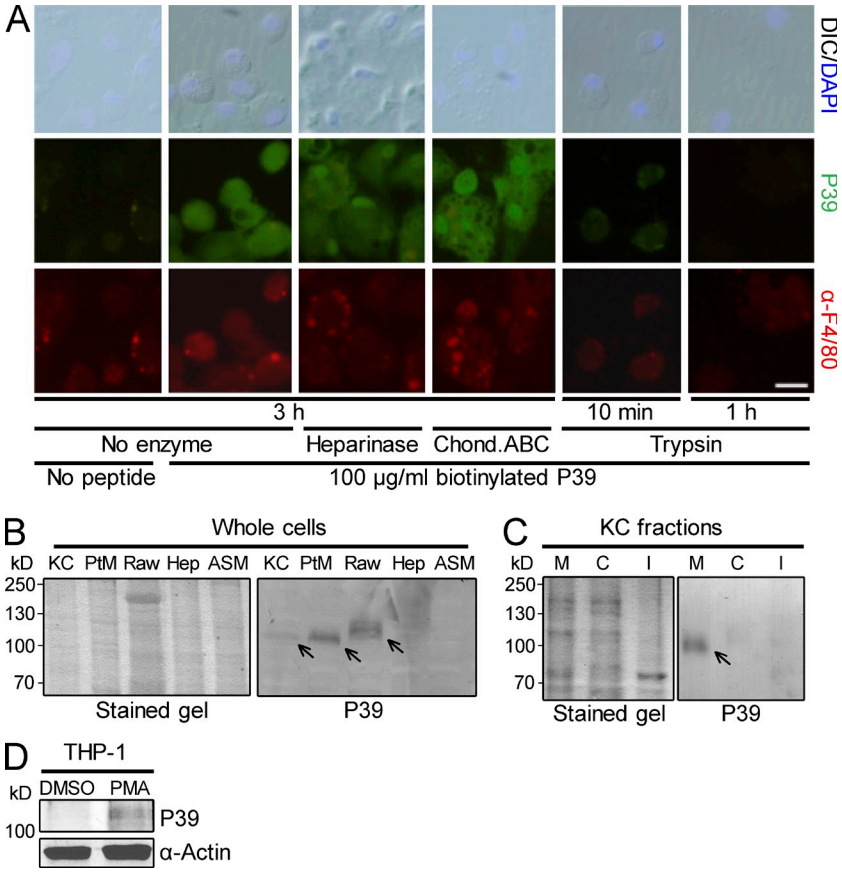

Figure 3. The P39 peptide binds to a macrophage-specific surface protein. (A) Primary Kupffer cells were incubated with heparinase I, chondroitinase ABC, or trypsin, as indicated. PBS buffer (no enzyme) served as a control. After enzyme treatment, 100 µg/ml biotinylated P39 peptide (green) and the anti-F4/80 antibody (red) were incubated for 1 h and visualized. The top row shows differential interference contrast (DIC) microscopy images merged with DAPI-stained nuclei (blue). P39 peptide binding was trypsin sensitive and unaffected by GAG-removing enzyme treatment. Bar, 20 µm. (B) Lysates from five different cell types were fractionated by gel electrophoresis, and binding of biotinylated P39 peptide to proteins on the blot was detected using alkaline phosphatase–conjugated streptavidin. KC, primary rat Kupffer cells; PtM, primary rat peritoneal macrophages; Raw, a mouse macrophage-like cell line; Hep, primary rat hepatocytes; ASM, primary rat airway smooth muscle cells. P39 peptide binding to an ~110-kD protein band (arrows) was detected only for the macrophage-like cells (rat KC, rat PtM, and mouse Raw). (C) Kupffer cell fractions were tested for P39 peptide binding. M, membrane fraction; C, cytosolic fraction; I, insoluble fraction. P39 peptide bound only to an ~110-kD membrane protein (arrow). (D) Activation of the human monocyte cell line THP-1 with PMA treatment for differentiation into a macrophage-like cell resulted in production of a protein recognized by the P39 peptide. No binding was detected for control THP-1 cells treated with DMSO carrier alone. An anti-actin antibody was used as a loading control. Immunofluorescence and far-Western blotting images are representative of two to three independent experiments.

binding protein to a subcellular compartment, primary rat Kupffer cells were fractionated into membrane, cytosolic, and insoluble fractions. As shown in Fig. 3 C, P39 binding to an ~110-kD band was detected only with the membrane fraction. We further verified the specificity of P39 peptide binding to macrophage membrane proteins by use of the human monocyte cell line THP-1, which can be induced to differentiate into macrophage-like cells by addition of PMA (Auwerx., 1991; Traore et al., 2005). P39 binding to an ~110-kD band was detected only after differentiation (Fig. 3 D).

In a separate set of experiments, we investigated whether inhibition of sporozoite entry was caused by peptide occupancy of a putative Kupffer cell receptor or, alternatively, by steric hindrance by the large (7-nm diameter × 1-µm length) phage particles. These experiments also aimed at assessing cell type specificity of peptide inhibition of sporozoite entry. A scrambled peptide with the same amino acid composition as P39, SC39, served as a negative control for these experiments (Fig. 4 A). As shown in Fig. 4 B, P39 did not bind significantly to hepatocytes, whereas binding to macrophage-like cells (Kupffer cells and THP-1) was strong. Binding was specific, as SC39 did not bind appreciably (Fig. 4 B). In agreement with the binding results, the P39 peptide significantly inhibited rodent *P. berghei* and human *Plasmodium falciparum* sporozoite entry into macrophage-like cells but not into primary rat hepatocytes or HepG2 human hepatoma cells (Fig. 4, C and D). The control SC39 peptide was not inhibitory (Fig. 4 D). Additional control experiments indicated that the P39 peptide does not influence macrophage phagocytic activity (not depicted), implying that the mechanism of inhibition of sporozoite entry is unrelated to phagocytic activity.

The P39 peptide binds to CD68, a putative receptor on the Kupffer cell surface

Far-Western blotting of Kupffer cell membrane proteins showed that the P39 peptide binds to a broad band ranging from ~110 to 120 kD (Fig. 5 A). Such broad bands are characteristic of heavily glycosylated proteins. To identify the protein to which the P39 peptide binds, we excised from a stained SDS-PAGE gel three pieces corresponding to the region of P39 binding (Fig. 5 B). The proteins in each of the pieces were analyzed by mass spectrometry and are listed at the bottom in Fig. 5 B. Two candidate glycoproteins, gp96 and CD68, were identified in two of the three fractions. Further tests indicated that CD68 expression is macrophage specific, whereas gp96 is not (Fig. 6, A and B). cDNA generated from

Cos7 cells was used as a negative control because the reactions used a heterologous, rat-specific primer set (Fig. 6 A). Western blotting and far-Western blotting assays showed that CD68 occurrence and P39 binding activity are both specific for macrophage-derived membrane proteins, whereas gp96 is not (Fig. 6 B). Even though Kupffer cells showed weaker gp96 mRNA expression, polyclonal anti-gp96 antibody detected a strong ~110-kD protein band on every cell type, suggesting that gp96 is a stable protein. The specificity of P39 peptide binding to CD68 was further verified by siRNA knockdown of CD68 expression, by CD68 ectopic expression by a nonmacrophage cell, and by glycosidase treatment (Fig. 6, C–E). siRNA treatment reduced CD68 mRNA abundance in primary rat Kupffer cells by ~85% (Fig. 6 C, left) and also abolished almost all detectable CD68 protein and P39 binding activity by day 6 after treatment (Fig. 6 C, right). The human 293T kidney cell line does not express CD68. These cells were engineered to express rat CD68 that lacks a transmembrane domain to promote secretion into the culture medium. 24 h after transfection, cells were washed with fresh RPMI medium lacking fetal bovine serum and incubated 2 d more to allow CD68 expression and secretion. Concentrated culture supernatants were used for CD68 detection. As shown in Fig. 6 D, supernatant from transfected, but not from nontransfected cells, contained CD68 protein as detected by anti-CD68 antibody and by P39 peptide binding. No significant binding was detected when the scrambled peptide was used. An equivalent amount of residual BSA (remaining after RPMI washing) was detected in transfected and nontransfected cell supernatants. CD68 is known to be a heavily glycosylated protein that is sensitive to *N*-glycosidase and insensitive to *O*-glycosidase (Van Velzen et al., 1997). When Kupffer cell membrane fraction was treated with *N*-glycosidase, CD68 gel electrophoretic mobility shifted from ~110 to ~80 kD, whereas no shift was observed after *O*-glycosidase treatment (Fig. 6 E). Significantly, a similar shift was observed for P39 binding activity (Fig. 6 E). Our model predicts that the putative CD68 receptor interacts with a sporozoite surface protein during sporozoite entry of Kupffer cells. To test this prediction, we incubated recombinant CD68 (Fig. 6 D) with *P. berghei* sporozoites and assayed binding by immunofluorescence and flow cytometry using an anti-CD68 antibody. As shown in Fig. 6 F, CD68 did indeed interact with the surface of sporozoites.

CD68 is a determinant of sporozoite cell entry

We tested the hypothesis that CD68 serves as a receptor for sporozoite cell entry in five different ways: (1) by inhibiting CD68 expression with siRNA, (2) by ectopic gene expression, (3) by gene overexpression, (4) by inducing differentiation into macrophage-like cells, and (5) by antibody inhibition experiments. CD68 expression and sporozoite cell entry were monitored by flow cytometry and by immunofluorescence assay (Fig. 7). In initial experiments, we treated primary Kupffer cells with either control siRNA or rat CD68 siRNA, followed by incubation with *P. berghei* sporozoites for 1 h.

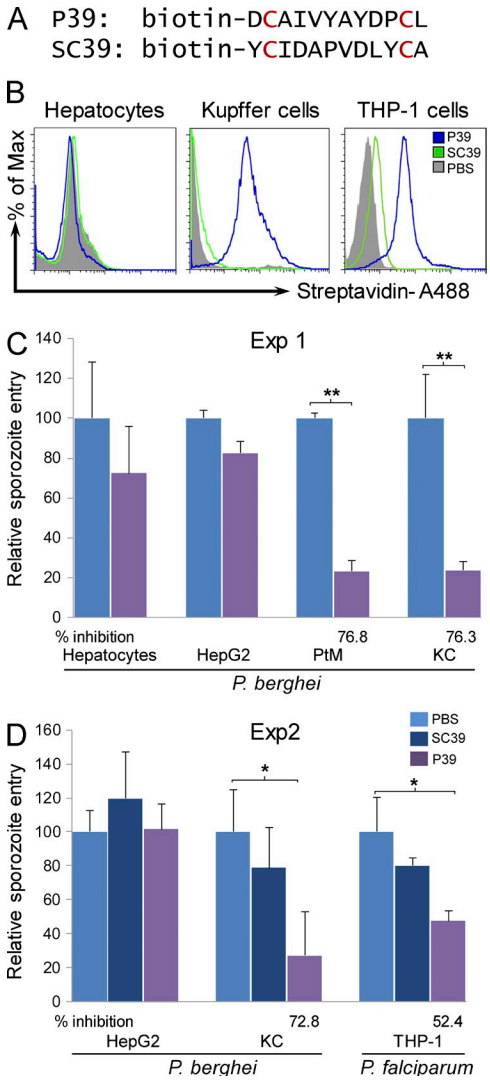

Figure 4. Specificity of P39 peptide binding and inhibition of sporozoite entry. (A) A scrambled peptide with the same amino acid composition as P39 (SC39) was designed to serve as a negative control. All peptides have a cysteine residue (red) at positions 2 and 11. (B) The cell type indicated at the top of each panel was incubated with buffer alone (PBS), with a biotinylated P39 peptide (P39), or with a biotinylated scrambled peptide (SC39), followed by incubation with fluorescent streptavidin and analysis by flow cytometry. The P39 peptide bound to macrophage-like cells (Kupffer, PMA-activated THP-1) but not to hepatocytes (Hep). The scrambled peptide did not bind appreciably to any of the cell types. All images are representative of two to three independent experiments. (C and D) Inhibition of sporozoite entry in vitro. (C) Each cell type was incubated with PBS alone or with the P39 peptide, before exposure to 2×10^4 *P. berghei* sporozoites. The mean number of internalized sporozoites per 20 microscopic fields/well under 400-fold magnification was determined, and the percent inhibition relative to the PBS-treated group is shown at the bottom of the figure. (D) The SC39 peptide was tested for inhibition of *P. berghei* and *P. falciparum* sporozoite entry into each cell type. P39 peptide and PBS treatments were used as positive and negative controls, respectively. (C and D) Data from three independent biological experiments were combined. P-values (*, $P < 0.05$; **, $P < 0.01$) were calculated using the one-way ANOVA test. Error bars indicate standard deviation.

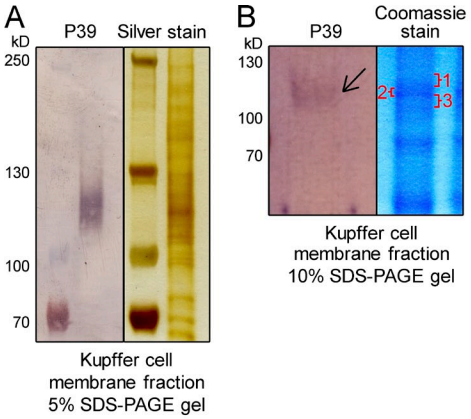

1	• Bile canaliculus-specific membrane glycoprotein precursor [*Rattus norvegicus*] • Oxoglutarate (alpha-ketoglutarate) dehydrogenase precursor [*Rattus norvegicus*] • Phosphate ABC transporter periplasmic substrate-binding protein PstS [*Serratia proteamaculans*] • **CD68 molecule** [*Rattus norvegicus*] • Glucosidase II [*Homo sapiens*] • Neutral alpha-glucosidase AB [*Rattus norvegicus*] • Bifunctional aconitate hydratase 2/2-methylisocitrate dehydratase [*Pseudomonas aeruginosa*] • Chaperonin GroEL [*Pseudomonas fluorescens* Pf-5]
2	• Tumor rejection antigen **gp96** [*Mus musculus*] • Mutant type II hexokinase [*Rattus norvegicus*] • Alpha actinin 4 [*Homo sapiens*] • Chaperonin GroEL [*Pseudomonas fluorescens* Pf-5] • Neutral alpha-glucosidase AB [*Rattus norvegicus*] • Phosphate ABC transporter periplasmic substrate-binding protein PstS [*Yersinia pestis* KIM] • Bile canaliculus-specific membrane glycoprotein precursor [*Rattus norvegicus*]
3	• PREDICTED: tumor rejection antigen (**gp96**) 1 isoform 6 [Pan troglodytes] • Actinin alpha 4 [*Mus musculus*] • Valosin containing protein [*Danio rerio*] • Procollagen-lysine, 2-oxoglutarate 5-dioxygenase 2, long variant [*Rattus norvegicus*] • Mutant type II hexokinase [*Rattus norvegicus*] • Phosphate ABC transporter periplasmic substrate-binding protein PstS [*Yersinia enterocolitica*] • Chaperone Hsp60, peptide-dependent ATPase, heat shock protein [*Pseudomonas fluorescens*] • Calnexin [*Cricetulus griseus*] • rCG60535, isoform CRA_b [*Rattus norvegicus*] • Glycine dehydrogenase [*Pseudomonas fluorescens* SBW25] • PREDICTED: similar to Ribosome-binding protein 1 [*Rattus norvegicus*] • **CD68 molecule** [*Rattus norvegicus*] • Elongation factor 2

Figure 5. The P39 peptide binds to ∼110–120-kD Kupffer cell membrane proteins. (A) Kupffer cell membrane proteins were fractionated by 5% SDS-PAGE and either used for far-Western blotting with the biotinylated P39 peptide (left) or stained with silver (right). P39 bound to a broad band of ∼110–120 kD, suggesting that it may bind to a glycosylated protein. Size markers were fractionated in the left lanes. (B) The P39 peptide–binding area (left, arrow) was excised in three pieces from a Coomassie blue–stained gel of rat Kupffer cell membrane fraction (numbered in red on the right). Each piece was analyzed by mass spectrometry, and the identified proteins are listed below. Two candidate glycoproteins that were identified in two fractions, gp96 and CD68, are highlighted in bold.

Sporozoite entry decreased from 19.4% for control Kupffer cells to 7.63% for CD68 siRNA–treated cells (Fig. 7 A). Next, nonmacrophage-like Cos7 cells were engineered for ectopic expression of the rat CD68, followed by incubation with *P. berghei* sporozoites for 1 h. Sporozoite entry increased from 1.91% for nonengineered cells to 2.23% for cells engineered with the CD68 expression construct (Fig. 7 B). The modest increase of sporozoite entry may be attributed to two factors: (1) it is likely that only a small proportion of the cells acquired the expression construct during transformation, and (2) CD68 functions as a scavenger receptor in macrophage-like cells (Ramprasad et al., 1996) and Cos7 cells lack other molecules involved in endocytosis. We therefore engineered the Raw macrophage-like cell line to overexpress rat CD68 and tested for sporozoite entry as described in Fig. 7 (A and B). As seen in Fig. 7 C, sporozoite entry changed from 5.24% in control cells to 10.03% in engineered cells. Next, we compared *P. falciparum* sporozoite entry into undifferentiated and differentiated THP-1 human macrophage-like cells. PMA treatment greatly increased CD68 expression and also increased *P. falciparum* sporozoite entry from 0.25 to 2.77% (Fig. 7 D). Finally, we preincubated primary rat Kupffer cells, mouse peritoneal macrophages, or activated THP-1 cells with corresponding rat, mouse, or human monoclonal anti-CD68 antibodies, followed by incubation with 2×10^4 sporozoites for 1 h. Anti-gp96, anti-F4/80, and anti-CD45 antibodies or no antibody served as controls. Each anti-CD68 antibody significantly inhibited sporozoite entry, whereas the control antibodies had no effect. Inhibition by anti–rat CD68 antibody (ED1) was ∼79.4%, by anti–mouse CD68 antibody (FA-11) was 34.6%, and by anti–human CD68 antibody (KP1) was 28.5% (Fig. 7 E). Differences in inhibition efficiencies may be caused by differences of the epitopes on the 110-kD CD68 molecule that are recognized by each monoclonal antibody.

We further tested the role of CD68 in infection of the liver with in vivo experiments using CD68 KO mutant mice (Song et al., 2011). PCR assays using genomic DNA extracted either from wild-type or CD68 KO mice confirmed the genotype of CD68 KO mice (Fig. 8 A), and Western blotting and immunofluorescence assays of peritoneal macrophages confirmed the lack of CD68 protein expression in CD68 KO mice (Fig. 8, B and C). KO macrophage phagocytic activity measured by fluorescent latex bead uptake was not affected by the mutation and was equal to that of wild-type macrophages (Fig. 8 D). Moreover, macrophages from CD68 KO mice have lost the preferential uptake of the P39 peptide observed with wild-type macrophages (Fig. 8 E). When incubated with *P. berghei* sporozoites, macrophages from CD68 KO mice showed ∼49% reduction of sporozoite entry compared with wild-type cells (Fig. 9 A). The hypothesis that CD68-expressing macrophages serve as an important gateway for *Plasmodium* sporozoite liver invasion in vivo was further tested by intravenous injection of *P. berghei* sporozoites into mice. Although parasite liver burden was ∼71% lower in CD68 KO mice than in wild-type mice (Fig. 9 B), blood stage infection showed no difference (Fig. 9 C). These results strongly suggest that decreased sporozoite entry into CD68 KO macrophages (Fig. 9 A) results in a large reduction of parasite liver burden in CD68 KO mice (Fig. 9 B). The 71% inhibition of parasite liver burden in CD68 KO mice (Fig. 9 B) correlated with a small but significant reduction of infection prevalence and increase of the prepatent time of infection when CD68 KO mice were infected by mosquito bites or by intravenous injection of *P. berghei* sporozoites (not depicted).

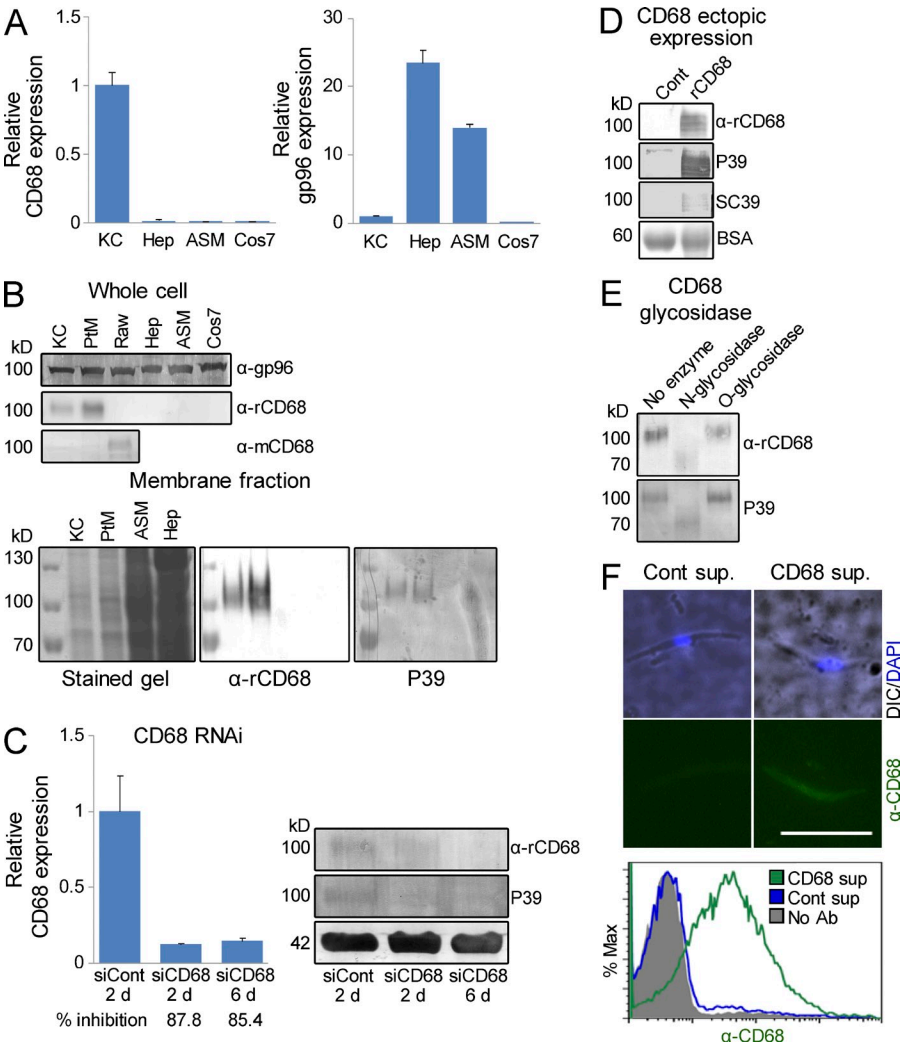

Figure 6. The P39 peptide binds to CD68, a molecule that mediates sporozoite entry into Kupffer cells. (A) qRT-PCR assays of primary rat Kupffer cells (KC), primary rat hepatocytes (Hep), primary rat airway smooth muscle cells (ASM), and a monkey kidney cell line (Cos7) show that CD68 is strongly expressed in Kupffer cells, whereas gp96 is not. Data were pooled from three experiments. (B, top) CD68 is a macrophage-specific membrane protein. Western blots of whole cell lysates were incubated either with anti-gp96 antibody or anti-CD68 antibody. (bottom) Western blots of membrane fractions were incubated with an anti-CD68 antibody or with the biotinylated P39 peptide. PtM, rat primary peritoneal macrophages; RAW, mouse macrophage-like cell line; α-rCD68, rat anti-CD68 antibody; α-mCD68, mouse anti-CD68 antibody. (C) CD68 siRNA treatment of rat Kupffer cells for 6 d inhibits CD68 protein expression as well as P39 peptide binding activity. (left) Relative CD68 mRNA expression in Kupffer cell culture was determined by qRT-PCR after the number of days of siRNA treatment indicated at the bottom. Data were combined from three independent experiments. (right) Western blot of membrane fraction probed with an anti-CD68 antibody or with biotinylated P39 peptide as indicated. An anti-actin antibody served to control loading. siCont, control siRNA of sequence unrelated to that of CD68. (A and C) Error bars indicate standard deviation. (D) The 293T cell line was engineered to express rat CD68 protein lacking the C-terminal transmembrane domain for secretion into the culture supernatant. Culture supernatant of control (not transfected) 293T cells and 293T cells that secrete rat CD68 was tested for binding of anti-CD68 antibody, biotinylated P39 peptide, or scrambled peptide. Residual BSA that remained after cells were washed with serum-free medium was detected by Ponceau staining. (E) Western blots of a rat Kupffer cell membrane fraction treated either with *N*-glycosidase or with *O*-glycosidase were incubated with anti-CD68 antibody or P39 peptide, as indicated. CD68 mobility was sensitive to *N*-glycosidase but not to *O*-glycosidase treatment. Images represent two independent experiments. (F) Purified *P. berghei* sporozoites were incubated with supernatant from either control 293T cells or from 293T cells engineered to secrete rat CD68 (compare with D). CD68 binding to sporozoites was visualized with an anti–rat CD68 antibody. Immunofluorescence images are representative of two independent experiments with five replicates each, and flow cytometry of sporozoites incubated with control or CD68-containing supernatant is representative of three independent experiments. DIC, differential interference contrast. Bar, 10 µm.

To confirm these observations, we used clodronate to deplete mice of Kupffer cells as described previously (Baer et al., 2007), followed by infection with injected *P. berghei* sporozoites (Fig. 9 D). Kupffer cell depletion made no significant difference in the liver burden of wild-type mice (Fig. 9 D, two left bars), whereas Kupffer cell depletion greatly increased liver infection of KO mice (Fig. 9 D, two right bars), indicating that in the absence of the CD68 receptor, Kupffer cells pose a significant barrier to liver infection. Kupffer cell depletion by clodronate was assessed quantitatively by measuring expression of the macrophage-specific gene *F4/80*. These data were compared with parasite liver burden using the Pearson's correlation coefficient. Although the percent reduction of F4/80-positive cells by clodronate treatment of wild-type and CD68 KO mice was similar (90.5 ± 11.5% and 88.2 ± 14.4%, respectively; Fig. 9 E), in wild-type mice the extent of liver infection was not correlated with the presence or absence of Kupffer cells (Fig. 9 E, left), whereas for KO mice removal of Kupffer cells greatly increased liver infection (Fig. 9 E, right). In summary, we show that expression of the CD68 protein on the surface of Kupffer cells is an important determinant of *Plasmodium* sporozoite liver invasion. The absence of CD68 on Kupffer cells of CD68 KO mice imposed a barrier for sporozoite liver invasion.

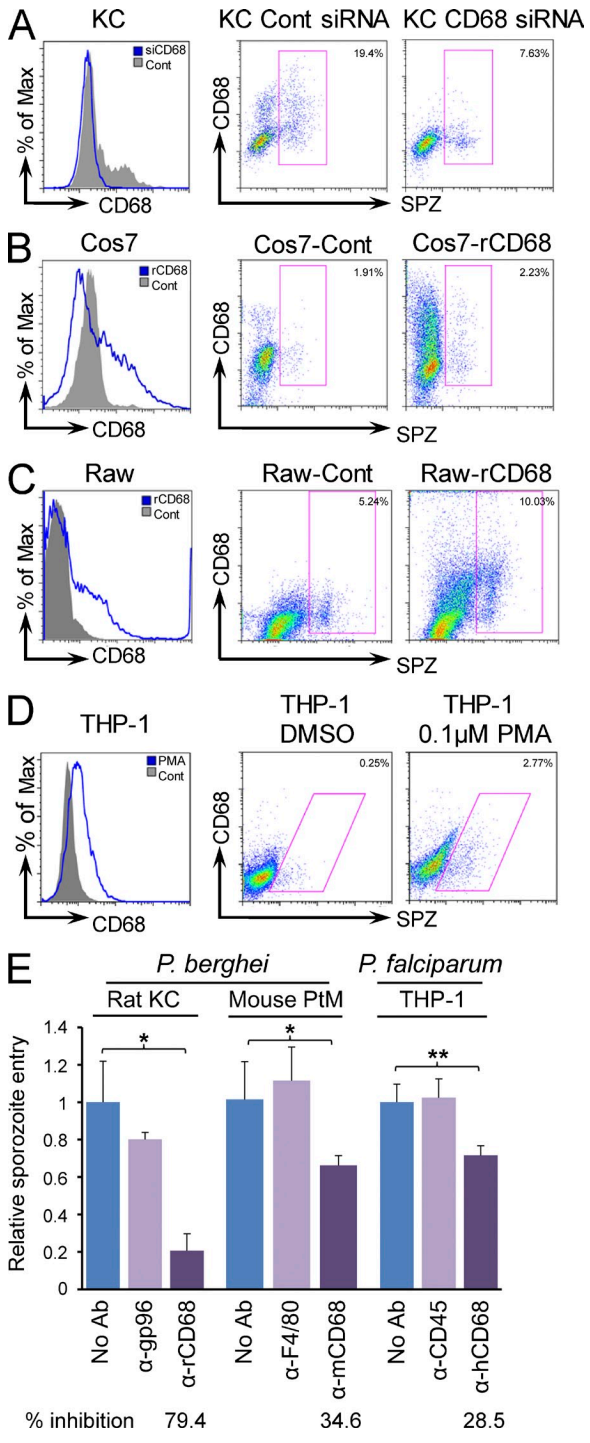

Figure 7. ***Plasmodium*** **sporozoites preferentially enter CD68-expressing cells.** (A) Primary rat Kupffer cells were incubated with CD68 siRNA to inhibit CD68 expression (compare with Fig. 6 C). 6 d after siRNA treatment, *P. berghei* sporozoites were added to either CD68 siRNA– or control siRNA–treated Kupffer cells. Parasite entry into host cells was determined by flow cytometry. Sporozoite-positive cells decreased from 19.4% in the control Kupffer cell population (Cont siRNA) to 7.63% in the CD68 siRNA–treated cells. CD68 was detected with an anti-CD68 antibody, whereas sporozoites were detected with an anti-CSP antibody. (B) A Cos7 monkey kidney cell line (Cos7-Cont) was engineered to express rat CD68 on its surface (Cos7-rCD68) and tested for *P. berghei* sporozoite entry by flow cytometry. Sporozoite-positive cells increased from 1.91% in the control population to 2.23% in the transfected Cos7 population. (C) A mouse Raw macrophage-like cell line (Raw-Cont) was engineered to express rat CD68 (Raw-rCD68) and tested for *P. berghei* sporozoite entry by flow cytometry. (D) A human monocyte THP-1 cell line was treated with 0.1 µM PMA to induce differentiation into macrophage-like cells and tested for *P. falciparum* sporozoite entry by flow cytometry. (E) Anti-CD68 antibody inhibits sporozoite entry into Kupffer cells and other CD68-expressing macrophages. Rat Kupffer cells (KC), mouse peritoneal macrophages (PtM), or activated THP-1 cells were preincubated with anti-CD68 antibody or control antibody as indicated. Relative sporozoite entry into host cell was determined at 2 h after incubation with 2×10^4 sporozoites per well. The percent inhibition of sporozoite entry compared with the control group (No antibody) is indicated. Data are from two independent experiments. *, $P < 0.05$; **, $P < 0.01$ (one-way ANOVA test). Error bars indicate standard deviation.

DISCUSSION

In the fight against malaria, the most effective points of control are the stages of parasite development at which the numbers are the lowest (bottlenecks). Fewer than 100 sporozoites are inoculated into a human by the bite of a mosquito (Kebaier et al., 2009), making preliver stages prime targets of control. Extensive evidence, mainly based on electron and confocal microscopy, suggests that Kupffer cells serve as the main gateway for sporozoite entry into the vertebrate liver parenchyma (Meis et al., 1983; Frevert et al., 2005, 2006; Baer et al., 2007). Sporozoite traversal of Kupffer cells involves active penetration and not phagocytosis (Vanderberg et al., 1990; Frevert et al., 2005), but little else is known about the molecular basis of this process. We screened a phage-based peptide library in an attempt to identify key molecules involved in Kupffer cell–sporozoite interactions. An attractive feature of this phage display approach is that it does not require any a priori knowledge of the interacting partner proteins. Furthermore, this approach is less prone to incorrect folding because it uses small 8–amino acid domains that are constrained by a cys-cys bond into a loop. The screen was successful in that starting with a highly complex library of $>10^9$ different peptides, close to half of the phages recovered after the screen displayed the same peptide (phage 39). Importantly, the three selected phages strongly inhibited sporozoite interactions with Kupffer cells both in vitro and in vivo, suggesting that the peptides displayed by the recombinant phages bound to a Kupffer cell receptor that is recognized by the sporozoite. We previously used the same peptide library to identify SM1, a peptide that binds to mosquito salivary glands and midgut epithelia and impairs parasite invasion of these tissues (Ghosh et al., 2001). These findings led to the identification of a receptor–ligand combination for sporozoite invasion of salivary glands (Ghosh et al., 2009) and a receptor–ligand combination for ookinete invasion of the midgut (Ghosh et al., 2011; Vega-Rodríguez et al., 2014).

Whereas interactions between CSP and liver GAGs are important for sporozoite recognition and attachment to the

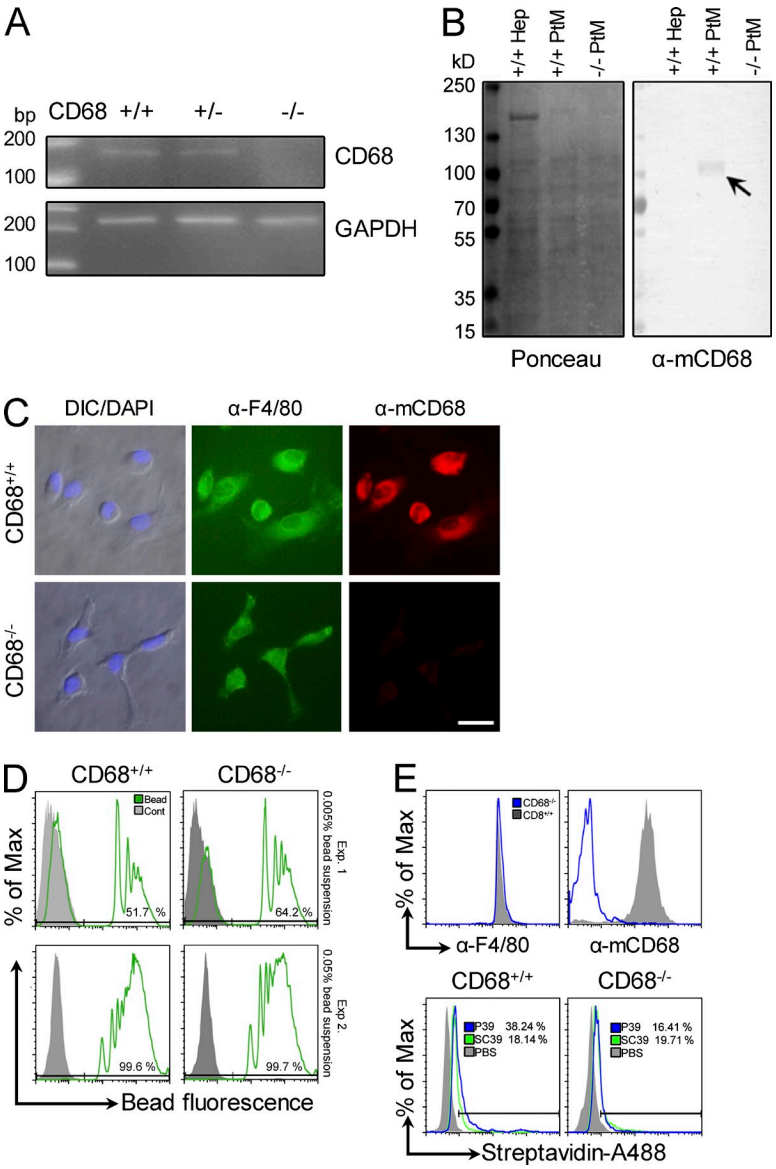

Figure 8. Characterization of wild-type and CD68 KO mice and their macrophages. (A) The genotype of the CD68 KO mice was confirmed using PCR with CD68-specific primers and mouse genomic DNA. +/+, wild-type mouse; +/−, heterozygous mouse; −/−, homozygous KO mouse. PCR with GAPDH primers served as a positive control. (B) Western blot of membrane proteins either stained (left) or incubated with an anti-CD68 antibody (right). Primary hepatocytes (Hep) served as a negative control. Arrow indicates CD68 signal in the +/+ lane. (C) Immunofluorescence assays of peritoneal macrophages from both wild-type and CD68 KO mice for anti-F4/80 expression. DIC, differential interference contrast. Bar, 20 µm. (D) Phagocytic activity of macrophages from CD68 KO mice. Flow cytometry results are shown for peritoneal macrophages incubated with two different fluorescent latex bead concentrations (Exp. 1 and Exp. 2 as indicated on the right of the figure). (E) KO macrophage recognition of the P39 peptide. Peritoneal macrophages from wild-type and CD68 KO mice were stained with the F4/80 antibody (recognizes macrophage-like cells) or an anti-CD68 antibody as indicated (top). The two cell types were also tested for uptake of the P39 peptide using the scrambled version, SC39, as a control (bottom). After incubation with the biotinylated peptides, cells were washed, fixed, and permeabilized for detection of intracellular peptide with Alexa Fluor 488–conjugated streptavidin. Data represent two independent experiments.

liver sinusoid, they are not essential for sporozoite–host cell recognition (Frevert et al., 1996). Kupffer cells also have different surface GAGs (Pradel et al., 2002) that in principle could serve as receptors and substrates for phage peptide binding. Therefore, we investigated whether inhibition of sporozoite entry by the selected phages involves GAGs on the Kupffer cell surface. The insensitivity of sporozoite entry to GAG removal from Kupffer cells and the trypsin sensitivity of peptide binding suggested that sporozoite entry occurs via interaction with a protein, a suggestion that was verified by the identification of CD68 as a P39-binding protein. Selective P39 peptide binding to the CD68 molecule on the Kupffer cell surface lends further support to the hypothesis that in vivo inhibition of sporozoite liver infection by the selected phages was caused by interference of Kupffer cell–sporozoite interactions.

The 71% reduction of parasite liver burden in CD68 KO mice strengthens the hypothesis that Kupffer cells serve as a major gateway for liver infection because in the liver these are the only cells that express CD68 on their surface. The observation that Kupffer cells in CD68 KO mice imposed a strong barrier for the sporozoite liver invasion, whereas CD68-expressing Kupffer cells in wild-type mice did not, strongly supports the gateway model. The observation that CD68 is especially abundant in phagocytic macrophages and low in cytokine-producing macrophages (Kinoshita et al., 2010), together with the finding that phagocytic macrophages mainly localize in the periportal area (Bykov et al., 2004), which is the area preferentially invaded by *Plasmodium* sporozoites (Meis et al., 1983), supports our observation.

It is not surprising that inhibition of sporozoite liver invasion by the peptide or in CD68 KO mice is not complete because not all Kupffer cells express CD68 (Kinoshita et al., 2010). Although CD68-positive Kupffer cells constitute the most abundant macrophage population in the liver, it is also

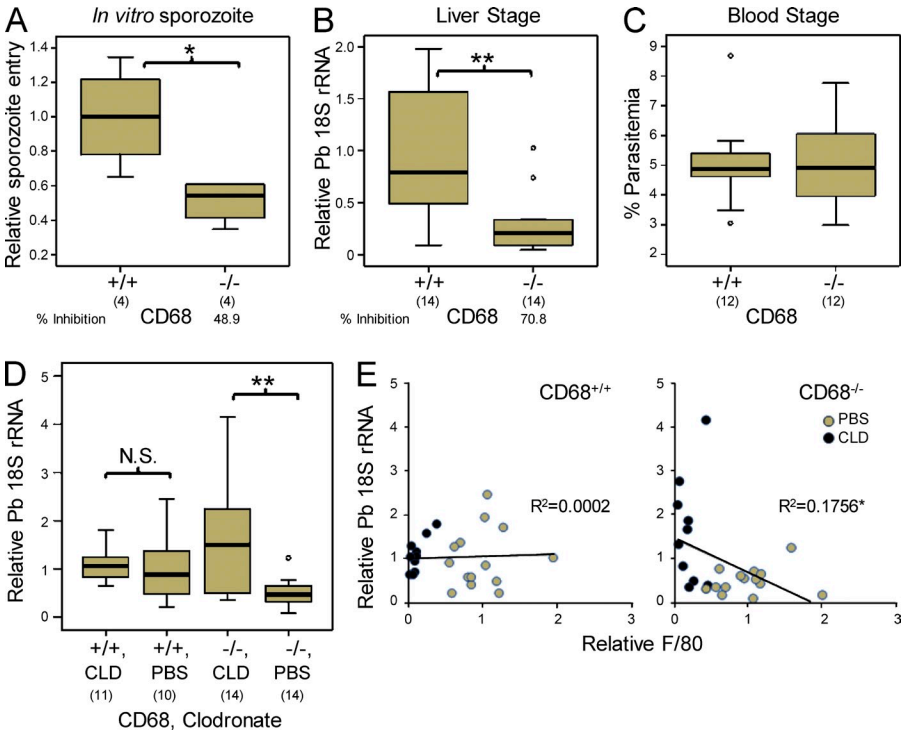

Figure 9. *P. berghei* sporozoite infection of CD68 KO mice is strongly impaired. (A) Primary cultures of peritoneal macrophages from wild-type mice (+/+) or from CD68 KO mice (−/−) were established in 8-well chamber slides, followed by incubation for 1 h with 2×10^4 *P. berghei* sporozoites per well. Parasite entry was determined as described previously (Pradel and Frevert, 2001). The graph shows the mean number of sporozoites per 20 fields/well under 400-fold magnification. Data are from two independent experiments, with 4 wells per experiment. A total of 8 wells (160 microscopic fields) were assayed for each genotype in the two experiments. (B) A total of 2×10^3 sporozoites were injected intravenously either into wild-type or CD68 KO mice. After 45 h, mice were sacrificed and liver parasite burden was determined by qRT-PCR. Data from three independent experiments were combined. (C) 2×10^3 *P. berghei*–infected red blood cells were injected intravenously either into wild-type mice or CD68 KO mice, and parasitemia was determined after 6 d. Data from two experiments were combined. (B and C) The total number of mice assayed is listed in parentheses under the genotype. (D) Wild-type (+/+) and CD68 KO mice (−/−) were injected either with clodronate liposomes (CLD) or with control liposomes produced with PBS, and after 2 d, 2×10^3 sporozoites were injected intravenously. 45 h after sporozoite injection, mice were sacrificed and the liver parasite burden was determined using qRT-PCR. The data from three independent experiments were combined. The total number of mice used for each type of assay is given in parentheses. (A–D) *, $P < 0.05$; **, $P < 0.01$. (E) Kupffer cell depletion by clodronate treatment was measured by relative expression of the *F4/80* gene in the liver. Pearson correlation efficiency between parasite liver burden and Kupffer cell depletion indicates that Kupffer cells in CD68 KO mice act as an invasion barrier, whereas this is not the case for wild-type mice. Open circles in B–D represent out-group data points. The data from three independent experiments were combined.

possible that sporozoites use alternative Kupffer cell receptors. Although we concentrated our efforts on the P39 peptide, the strongest binder, our phage display library screening against primary rat Kupffer cells identified two peptides in addition to P39. The P61 peptide binds to rat CD68 strongly but binds weaker to human CD68 (unpublished data). The P52 peptide may bind to other putative Kupffer cell receptors or alternatively bind to other domains of the CD68 protein. Furthermore, as shown by Tavares et al. (2013), sporozoites may also exit the sinusoid by traversal of endothelial cells, a process expected to be insensitive to peptide inhibition or to the absence of the CD68 putative receptor. They found ∼17% of events of sporozoite sinusoidal traversal were directly through endothelial cells without Kupffer cell involvement.

CD68 is a heavily glycosylated membrane protein, a member of the Lamp/lgp family. The protein has a predicted molecular mass of ∼35 kD but reaches 87–115 kD when fully glycosylated (Holness et al., 1993). This extensive *O*-glycosylation was proposed to protect the core protein and other closely associated membrane proteins from enzyme attack in the lysosome lumen (Holness et al., 1993). As such, *Plasmodium* sporozoites may take advantage of being enclosed by a heavily glycosylated CD68 endosome for protection from lysosomal enzyme attack within the Kupffer cell. Another layer of sporozoite protection may be afforded by triggering the inhibition of Kupffer cell respiratory burst via sporozoite CSP and Kupffer cell low-density lipoprotein receptor–related protein (LRP-1) interaction (Usynin et al., 2007). Previous findings suggest that inhibition of phagocytosis with silica treatment inhibits sporozoite clearance from the blood circulation (Verhave et al., 1980). Moreover, sporozoites within Kupffer cells appear to be surrounded by pseudopods that in turn associate with microfilaments, suggesting phagocytic enclosure of sporozoites (Meis et al., 1983). *Plasmodium* sporozoites may take advantage of the rapid CD68 scavenging as a shuttle to traverse Kupffer cells and move toward liver parenchyma (Ramprasad et al., 1996; Kurushima et al., 2000). This hypothesis is not supported by the previous work (Pradel and Frevert, 2001), which showed that in vitro inhibition of Kupffer cell phagocytosis by gadolinium chloride did not inhibit sporozoite Kupffer cell entry. However we found that P39 internalization by Kupffer cells was inhibited not by gadolinium chloride but by silica treatment (unpublished data). Our findings provide vital new insights on the molecular mechanisms for sporozoite egress from the blood circulation to establish infection of the liver. Identification of the sporozoite

ligand or ligands that interact with CD68 may lead to the discovery of new antigens for improved formulation of a pre-erythrocytic vaccine.

MATERIALS AND METHODS

Cell culture and sporozoite isolation. Isolation and primary culture procedures of rat Kupffer cells were as described previously (Pradel and Frevert, 2001). In brief, livers of ∼225–250-g male Sprague Dawley rats were perfused through portal vein with 0.05% collagenase type IV for 15 min at 37°C. After perfusion, liver cells were dissociated and further separated by a two-step Percoll (50 and 25%) gradient. Kupffer cells were recovered from the bottom layer (50% Percoll) and further enriched by subsequent ex vivo culture for 7 d. All procedures were executed in accordance with a protocol approved by the Johns Hopkins University Animal Care and Use Committee. Cells were cultured in RPMI medium supplemented with 10% fetal bovine serum. THP-1 human monocyte cells were activated to develop into macrophage-like cells by treatment with PMA (Sigma-Aldrich; 1,000-fold dilution of a 0.1 mM stock in DMSO) for 4 d. Control groups received the same amount of DMSO (Auwerx, 1991; Traore et al., 2005).

Sporozoites were isolated from infected *Anopheles stephensi* mosquitoes using dissection or density gradient centrifugation. For density gradient centrifugation, heads/thoraces (containing salivary glands) of infected female mosquitos were collected and homogenized in 10 ml RPMI medium with 5% fetal bovine serum. After centrifuging at 85 *g* for 5 min, the supernatant was further centrifuged at 16,500 *g* (RC6+ with HB6 rotor; Sorval) for 10 min. The pellet was resuspended with 3 ml RPMI medium and layered on OptiPrep (Sigma-Aldrich) density gradient medium, 6 ml of 15.42% bottom and 6 ml of 10.2% top. After centrifugation at 16,500 *g* for 10 min, sporozoites were recovered from the top of the 10.2% layer.

CD68 KO mouse. A CD68 KO mouse was originally generated and reported by Song et al. (2011). This mouse was transferred to Johns Hopkins Bloomberg School of Public Health and maintained under a protocol approved by the Johns Hopkins University Animal Care and Use Committee. The CD68 KO mice had been backcrossed seven generations to the C57B1/6J background. A wild-type control mouse line was isolated from F_2 littermates and used as a control.

Immunofluorescence assay and in vitro sporozoite entry inhibition. Cultured cells or sporozoites were fixed in 4% paraformaldehyde in PBS for 30 min and blocked with 4% BSA in PBS for 1 h. Rat Kupffer cell purity in primary cell cultures was determined with anti-F4/80 antibody (Santa Cruz Biotechnology, Inc.). For the in vitro sporozoite entry inhibition assays, each cell type was preincubated with a total of 10^9 phages (Bonnycastle et al., 1996) or 80 µg peptide or 10 µg antibody (anti–rat CD68 [ED1; AbD Serotec], anti–mouse CD68 [FA-11; eBioscience], anti–human CD68 [KP1; BioLegend], anti-gp96 antibody [Sigma-Aldrich], anti–mouse F4/80 [eBioscience], or anti–human CD45 [BioLegend]) in 200 µl medium per well (8-well chamber slides; Lab-Tek II) for 10 min, followed by addition of 2×10^4 sporozoites for 2 h. Sporozoite double-labeling procedure to distinguish between attached and internalized sporozoites was slightly modified from the previously described procedure (Pradel and Frevert, 2001). In brief, attached sporozoites were incubated with an anti-CSP antibody (Yoshida et al., 1980), followed by incubation with a rhodamine-conjugated (red) secondary antibody (Invitrogen). After 0.2% Triton X treatment for permeabilization, internalized sporozoites were detected by incubation with the same anti-CSP antibody, followed by incubation with an Alexa Fluor 488–conjugated (green) secondary antibody (Invitrogen). At the end of the procedure, internalized sporozoites fluoresce green and surface sporozoites fluoresce orange.

Enzyme treatment of Kupffer cells. GAG removal was performed as described previously (Pradel et al., 2002). In brief, primary cultures were treated with heparinase (20 mU/ml), chondroitinase ABC (500 mU/ml), or both for 4 h at 37°C. Trypsin treatment was as indicated in Fig. 3 A. *N*- or *O*-glycosidase treatment of Kupffer cell membrane fraction was as per the manufacturer's directions (060M0724; Sigma-Aldrich).

Western and far-Western blotting assay. Cells from in vitro cultures ($1 \sim 2 \times 10^7$ cells) were harvested, pelleted, resuspended with 1× SDS gel loading buffer, and boiled for 10 min. For cell fractionation, $\sim 1–2 \times 10^7$ rat primary Kupffer cells were harvested with buffer 1 (0.01% digitonin, 10 mM PIPES, pH 6.8, 300 mM Sucrose, 100 mM NaCl, 3 mM $MgCl_2$, and 5 mM EDTA) and rotated for 10 min at 4°C. After 1-min centrifugation (16,900 *g*), the supernatant (cytosolic fraction) was collected and the cell pellet was washed with buffer 1. The pellet was then resuspended with buffer 2 (0.5% Triton X-100, 10 mM PIPES, pH 7.4, 300 mM Sucrose, 100 mM NaCl, 3 mM $MgCl_2$, and 3 mM EDTA) and rotated for 20 min at 4°C. After 1-min centrifugation (16,900 *g*), the supernatant (membrane fraction) was collected and the cell pellet was washed with buffer 2. The pellet was then resuspended in 6.5 M urea (insoluble fraction). Protein lysates were separated in 10% SDS-PAGE gel and then stained with Coomassie dye or transferred onto a polyvinylidene fluoride membrane. Membranes were incubated for 1 h in blocking buffer (0.1% Tween 20 and 5% milk in PBS), followed by addition of a primary antibody or 0.5 mg/ml synthetic peptide. Specific antibody (anti–rat CD68 [AbD Serotec], anti–mouse and –human CD68 [eBioscience], and anti-gp96 [Sigma-Aldrich]) or peptide binding was visualized with alkaline phosphatase–conjugated secondary antibodies (Promega) or phosphatase-conjugated streptavidin (EMD Millipore), respectively.

P39 peptide and scrambled P39. P39, biotin-DCAIVYAYDPCL (Bio-Synthesis, Inc.), and scrambled P39, with the same amino acid composition as P39 but with a different amino acid sequence, biotin-YCIDAPVDLYCA (GenScript), were synthesized and further processed for circularization by formation of a disulfide bond between two cysteines in positions 2 and 11, resulting in the formation of an 8–amino acid loop (Fig. 1 A).

Flow cytometry assays. For the peptide binding assay, 5×10^5 cells were harvested and fixed in 4% paraformaldehyde for 15 min at 4°C. After triple washing, each cell pellet was resuspended in 100 µl PBS. Macrophage-like cells were initially treated with an Fc receptor–blocking antibody (eBioscience) for 10 min. This was followed by addition of 1 µl of 2 mg/ml *N*′-biotinylated synthetic peptide P39, *N*′-biotinylated scrambled P39, or PBS as a control to 100 µl of cell suspension and incubation for 30 min at 4°C. Alexa Fluor 488–conjugated streptavidin (Invitrogen) was then added and incubated for a further 30 min to detect peptides bound to each cell type. For the phagocytosis assay, 5×10^5 cells were harvested and incubated with fluorescent latex beads (L8530; Sigma-Aldrich) or *N*′-biotinylated synthetic peptides for 20 min, followed by fixation and further permeabilization for the detection of intracellular peptide uptake. For the sporozoite entry assay, $5–10 \times 10^5$ cells were harvested and incubated in 37°C with the same number of sporozoites. After 1-h incubation, cells were washed, fixed, and permeabilized for sporozoite detection using PE-conjugated anti-CSP antibody. APC-conjugated anti-CD68 antibody (eBioscience) and Alexa Fluor 488–conjugated anti-F4/80 antibody (eBioscience) were used for detection of CD68 and F4/80, respectively. FACS data were acquired with a FACSCalibur apparatus (BD) and analyzed using the FlowJo v8.7 software (Tree Star).

Manipulation of the CD68 expression. CD68 expression in the primary rat Kupffer cell was inhibited by transfecting CD68 siRNA (4390771; Ambion). Control siRNA (4390843; Ambion) was used for a negative control. In brief, CD68 siRNA or control siRNA was mixed with Lipofectamine RNAiMAX (Invitrogen) and added to a rat primary culture. Relative expression of CD68 was determined 2 and 6 d after treatment. The GFP expression cassette of the pMaxGFP (Amaxa) plasmid was substituted with the rat CD68 coding sequence (GenBank accession no. NM_001031638), using restriction enzymes KpnI and XhoI, and transfected into target cells using Xfect transfection reagent (Takara Bio Inc.). Expression of CD68 was determined either with Western blotting assay or flow cytometry.

Statistics for data analysis. The one-way ANOVA test or Mann-Whitney *U* test was used to compare the means of three biological replicates of each experimental group. Error bars indicate standard deviation.

The filamentous M13 (f88.4) phage library used in this work was kindly provided by Dr. Jamie K. Scott from Simon Fraser University, Burnaby, British Columbia, Canada. We thank the Johns Hopkins Malaria Research Institute mosquito and parasite core facilities for help with mosquito rearing and with *P. falciparum* gametocyte culture. Support from the Johns Hopkins Malaria Research Institute and the Bloomberg Family Foundation is gratefully acknowledged.

This work was supported by grant AI080668 from the National Institute of Allergy and Infectious Diseases (NIAID). Supply of human blood was supported by National Institutes of Health grant RR00052.

The authors declare no competing financial interests.

Submitted: 23 March 2011
Accepted: 2 July 2015

REFERENCES

Auwerx, J. 1991. The human leukemia cell line, THP-1: a multifacetted model for the study of monocyte-macrophage differentiation. *Experientia*. 47:22–31. http://dx.doi.org/10.1007/BF02041244

Baer, K., M. Roosevelt, A.B. Clarkson Jr., N. van Rooijen, T. Schnieder, and U. Frevert. 2007. Kupffer cells are obligatory for *Plasmodium yoelii* sporozoite infection of the liver. *Cell. Microbiol.* 9:397–412. http://dx.doi.org/10.1111/j.1462-5822.2006.00798.x

Bonnycastle, L.L., J.S. Mehroke, M. Rashed, X. Gong, and J.K. Scott. 1996. Probing the basis of antibody reactivity with a panel of constrained peptide libraries displayed by filamentous phage. *J. Mol. Biol.* 258:747–762. http://dx.doi.org/10.1006/jmbi.1996.0284

Bruña-Romero, O., J.C. Hafalla, G. González-Aseguinolaza, G. Sano, M. Tsuji, and F. Zavala. 2001. Detection of malaria liver-stages in mice infected through the bite of a single *Anopheles* mosquito using a highly sensitive real-time PCR. *Int. J. Parasitol.* 31:1499–1502. http://dx.doi.org/10.1016/S0020-7519(01)00265-X

Bykov, I., P. Ylipaasto, L. Eerola, and K.O. Lindros. 2004. Functional differences between periportal and perivenous Kupffer cells isolated by digitonin-collagenase perfusion. *Comp. Hepatol.* 3:S34. http://dx.doi.org/10.1186/1476-5926-2-S1-S34

Cerami, C., U. Frevert, P. Sinnis, B. Takacs, and V. Nussenzweig. 1994. Rapid clearance of malaria circumsporozoite protein (CS) by hepatocytes. *J. Exp. Med.* 179:695–701. http://dx.doi.org/10.1084/jem.179.2.695

Coppi, A., R. Tewari, J.R. Bishop, B.L. Bennett, R. Lawrence, J.D. Esko, O. Billker, and P. Sinnis. 2007. Heparan sulfate proteoglycans provide a signal to *Plasmodium* sporozoites to stop migrating and productively invade host cells. *Cell Host Microbe*. 2:316–327. http://dx.doi.org/10.1016/j.chom.2007.10.002

Danforth, H.D., M. Aikawa, A.H. Cochrane, and R.S. Nussenzweig. 1980. Sporozoites of mammalian malaria: attachment to, interiorization and fate within macrophages. *J. Protozool.* 27:193–202. http://dx.doi.org/10.1111/j.1550-7408.1980.tb04680.x

Frevert, U., P. Sinnis, C. Cerami, W. Shreffler, B. Takacs, and V. Nussenzweig. 1993. Malaria circumsporozoite protein binds to heparan sulfate proteoglycans associated with the surface membrane of hepatocytes. *J. Exp. Med.* 177:1287–1298. http://dx.doi.org/10.1084/jem.177.5.1287

Frevert, U., P. Sinnis, J.D. Esko, and V. Nussenzweig. 1996. Cell surface glycosaminoglycans are not obligatory for *Plasmodium berghei* sporozoite invasion in vitro. *Mol. Biochem. Parasitol.* 76:257–266. http://dx.doi.org/10.1016/0166-6851(95)02563-4

Frevert, U., S. Engelmann, S. Zougbédé, J. Stange, B. Ng, K. Matuschewski, L. Liebes, and H. Yee. 2005. Intravital observation of *Plasmodium berghei* sporozoite infection of the liver. *PLoS Biol.* 3:e192. http://dx.doi.org/10.1371/journal.pbio.0030192

Frevert, U., I. Usynin, K. Baer, and C. Klotz. 2006. Nomadic or sessile: can Kupffer cells function as portals for malaria sporozoites to the liver? *Cell. Microbiol.* 8:1537–1546. http://dx.doi.org/10.1111/j.1462-5822.2006.00777.x

Ghosh, A.K., P.E. Ribolla, and M. Jacobs-Lorena. 2001. Targeting *Plasmodium* ligands on mosquito salivary glands and midgut with a phage display peptide library. *Proc. Natl. Acad. Sci. USA*. 98:13278–13281. http://dx.doi.org/10.1073/pnas.241491198

Ghosh, A.K., M. Devenport, D. Jethwaney, D.E. Kalume, A. Pandey, V.E. Anderson, A.A. Sultan, N. Kumar, and M. Jacobs-Lorena. 2009. Malaria parasite invasion of the mosquito salivary gland requires interaction between the *Plasmodium* TRAP and the *Anopheles* saglin proteins. *PLoS Pathog.* 5:e1000265. http://dx.doi.org/10.1371/journal.ppat.1000265

Ghosh, A.K., I. Coppens, H. Gårdsvoll, M. Ploug, and M. Jacobs-Lorena. 2011. *Plasmodium* ookinetes coopt mammalian plasminogen to invade the mosquito midgut. *Proc. Natl. Acad. Sci. USA*. 108:17153–17158. http://dx.doi.org/10.1073/pnas.1103657108

Holness, C.L., R.P. da Silva, J. Fawcett, S. Gordon, and D.L. Simmons. 1993. Macrosialin, a mouse macrophage-restricted glycoprotein, is a member of the lamp/lgp family. *J. Biol. Chem.* 268:9661–9666.

Ito, J., A. Ghosh, L.A. Moreira, E.A. Wimmer, and M. Jacobs-Lorena. 2002. Transgenic anopheline mosquitoes impaired in transmission of a malaria parasite. *Nature*. 417:452–455. http://dx.doi.org/10.1038/417452a

Kebaier, C., T. Voza, and J. Vanderberg. 2009. Kinetics of mosquito-injected *Plasmodium* sporozoites in mice: fewer sporozoites are injected into sporozoite-immunized mice. *PLoS Pathog.* 5:e1000399. http://dx.doi.org/10.1371/journal.ppat.1000399

Kinoshita, M., T. Uchida, A. Sato, M. Nakashima, H. Nakashima, S. Shono, Y. Habu, H. Miyazaki, S. Hiroi, and S. Seki. 2010. Characterization of two F4/80-positive Kupffer cell subsets by their function and phenotype in mice. *J. Hepatol.* 53:903–910. http://dx.doi.org/10.1016/j.jhep.2010.04.037

Kurushima, H., M. Ramprasad, N. Kondratenko, D.M. Foster, O. Quehenberger, and D. Steinberg. 2000. Surface expression and rapid internalization of macrosialin (mouse CD68) on elicited mouse peritoneal macrophages. *J. Leukoc. Biol.* 67:104–108.

Meis, J.F., J.P. Verhave, P.H. Jap, and J.H. Meuwissen. 1983. An ultrastructural study on the role of Kupffer cells in the process of infection by *Plasmodium berghei* sporozoites in rats. *Parasitology*. 86:231–242. http://dx.doi.org/10.1017/S003118200005040X

Moorthy, V.S., and M.P. Kieny. 2010. Reducing empiricism in malaria vaccine design. *Lancet Infect. Dis.* 10:204–211. http://dx.doi.org/10.1016/S1473-3099(09)70329-9

Moorthy, V.S., M.F. Good, and A.V. Hill. 2004. Malaria vaccine developments. *Lancet*. 363:150–156. http://dx.doi.org/10.1016/S0140-6736(03)15267-1

Pinzon-Ortiz, C., J. Friedman, J. Esko, and P. Sinnis. 2001. The binding of the circumsporozoite protein to cell surface heparan sulfate proteoglycans is required for *Plasmodium* sporozoite attachment to target cells. *J. Biol. Chem.* 276:26784–26791. http://dx.doi.org/10.1074/jbc.M104038200

Pradel, G., and U. Frevert. 2001. Malaria sporozoites actively enter and pass through rat Kupffer cells prior to hepatocyte invasion. *Hepatology*. 33:1154–1165. http://dx.doi.org/10.1053/jhep.2001.24237

Pradel, G., S. Garapaty, and U. Frevert. 2002. Proteoglycans mediate malaria sporozoite targeting to the liver. *Mol. Microbiol.* 45:637–651. http://dx.doi.org/10.1046/j.1365-2958.2002.03057.x

Ramprasad, M.P., V. Terpstra, N. Kondratenko, O. Quehenberger, and D. Steinberg. 1996. Cell surface expression of mouse macrosialin and human CD68 and their role as macrophage receptors for oxidized low density lipoprotein. *Proc. Natl. Acad. Sci. USA*. 93:14833–14838. http://dx.doi.org/10.1073/pnas.93.25.14833

Song, L., C. Lee, and C. Schindler. 2011. Deletion of the murine scavenger receptor CD68. *J. Lipid Res.* 52:1542–1550. http://dx.doi.org/10.1194/jlr.M015412

Sturm, A., R. Amino, C. van de Sand, T. Regen, S. Retzlaff, A. Rennenberg, A. Krueger, J.M. Pollok, R. Menard, and V.T. Heussler. 2006. Manipulation of host hepatocytes by the malaria parasite for delivery into liver sinusoids. *Science*. 313:1287–1290. http://dx.doi.org/10.1126/science.1129720

Tavares, J., P. Formaglio, S. Thiberge, E. Mordelet, N. Van Rooijen, A. Medvinsky, R. Ménard, and R. Amino. 2013. Role of host cell traversal by the malaria sporozoite during liver infection. *J. Exp. Med.* 210:905–915. http://dx.doi.org/10.1084/jem.20121130

Traore, K., M.A. Trush, M. George Jr., E.W. Spannhake, W. Anderson, and A. Asseffa. 2005. Signal transduction of phorbol 12-myristate 13-acetate (PMA)-induced growth inhibition of human monocytic leukemia THP-1 cells is reactive oxygen dependent. *Leuk. Res.* 29:863–879. http://dx.doi.org/10.1016/j.leukres.2004.12.011

Usynin, I., C. Klotz, and U. Frevert. 2007. Malaria circumsporozoite protein inhibits the respiratory burst in Kupffer cells. *Cell. Microbiol.* 9:2610–2628. http://dx.doi.org/10.1111/j.1462-5822.2007.00982.x

Van Velzen, A.G., R.P. Da Silva, S. Gordon, and T.J. Van Berkel. 1997. Characterization of a receptor for oxidized low-density lipoproteins on rat Kupffer cells: similarity to macrosialin. *Biochem. J.* 322:411–415.

Vanderberg, J.P., S. Chew, and M.J. Stewart. 1990. *Plasmodium* sporozoite interactions with macrophages in vitro: a videomicroscopic analysis. *J. Protozool.* 37:528–536. http://dx.doi.org/10.1111/j.1550-7408.1990.tb01260.x

Vega-Rodríguez, J., A.K. Ghosh, S.M. Kanzok, R.R. Dinglasan, S. Wang, N.J. Bongio, D.E. Kalume, K. Miura, C.A. Long, A. Pandey, and M. Jacobs-Lorena. 2014. Multiple pathways for *Plasmodium* ookinete invasion of the mosquito midgut. *Proc. Natl. Acad. Sci. USA.* 111:E492–E500. http://dx.doi.org/10.1073/pnas.1315517111

Verhave, J.P., J.H. Meuwissen, and J. Golenser. 1980. The dual role of macrophages in the sporozoite-induced malaria infection. A hypothesis. *Int. J. Nucl. Med. Biol.* 7:149–156. http://dx.doi.org/10.1016/0047-0740(80)90033-9

Vreden, S.G. 1994. The role of Kupffer cells in the clearance of malaria sporozoites from the circulation. *Parasitol. Today (Regul. Ed.).* 10:304–308. http://dx.doi.org/10.1016/0169-4758(94)90084-1

White, N.J., S. Pukrittayakamee, T.T. Hien, M.A. Faiz, O.A. Mokuolu, and A.M. Dondorp. 2014. Malaria. *Lancet.* 383:723–735. http://dx.doi.org/10.1016/S0140-6736(13)60024-0

Widmann, J.J., R.S. Cotran, and H.D. Fahimi. 1972. Mononuclear phagocytes (Kupffer cells) and endothelial cells. Identification of two functional cell types in rat liver sinusoids by endogenous peroxidase activity. *J. Cell Biol.* 52:159–170. http://dx.doi.org/10.1083/jcb.52.1.159

Yoshida, N., R.S. Nussenzweig, P. Potocnjak, V. Nussenzweig, and M. Aikawa. 1980. Hybridoma produces protective antibodies directed against the sporozoite stage of malaria parasite. *Science.* 207:71–73. http://dx.doi.org/10.1126/science.6985745